RSC Advances

PAPER

View Article Online
View Journal | View Issue

Cite this: *RSC Adv.*, 2017, **7**, 22541

NiX_2 (X = Cl and Br) sheets as promising spin materials: a first-principles study†

Muhammad Mushtaq, Yungang Zhou* and Xia Xiang*

Received 22nd February 2017
Accepted 7th April 2017

DOI: 10.1039/c7ra02218b

rsc.li/rsc-advances

In order to achieve paper-like spin devices, it is rather critical to develop new two-dimensional (2D) spin materials. In this study, the geometrical structure, stability, and electronic and magnetic properties of 2D nickel dihalides of NiX_2 (X = Cl and Br) type were investigated using density functional theory (DFT) calculations. We found that after optimization, geometries of $NiCl_2$ and $NiBr_2$ sheets that are obtained from their bulk counterparts are well kept. Phonon dispersion calculations demonstrated that both $NiCl_2$ and $NiBr_2$ sheets are dynamically stable. Magnetism calculations showed that ferromagnetic (FM) coupling is ground state for both structures in which per $NiCl_2$ and $NiBr_2$ unit cells can possess the moments of 1.91 and 1.88 μ_B, respectively. Density of states (DOS) and band structure calculations revealed that both structures are magnetic semiconductors with large band gaps. In addition, strain effect also showed that the moments of $NiCl_2$ and $NiBr_2$ sheets can be effectively tuned by applying the biaxial strain. A unique combination of integrated geometry, dynamical stability, intrinsic ferromagnetism, a magnetic semiconductor and tunable magnetism makes $NiCl_2$ and $NiBr_2$ sheets promising candidates for next-generation paper-like spin devices.

Introduction

Driven by the enormous demand of the microprocessor market all over the world, a paper-like spin device has become one of the most exciting and challenging research areas. Paper-like spin devices can not only utilize spin degree of freedom of the electron to sense, store, process and transfer information with high density and high sensitivity but can also overcome the fundamental limits, such as heat dissipation and energy loss, of the device architecture caused by the diminishing size of the devices in current semiconductor technologies. Thus, the development of paper-like spin devices is important to both fundamental scientific research and industrial applications. It is well known that the performance of a device strongly depends on the properties of the material. Consequently, the progress of paper-like spin devices drives us to further develop advanced 2D spin materials.

Thus far, different families of 2D materials, such as the group IVA family (graphene, silicene and germanene),[1,2] group IIIA (boronene),[3] group VA family (phosphorene, arsenene and antimonene),[4,5] group IIIA–VA family (BN sheet),[6,7] group IVA–VIA family (GeS, GeSe, SnS and SnSe sheets),[8] transition metal dichalcogenides (MoS_2, $MoSe_2$, WS_2, WSe_2, TaS_2, $TaSe_2$, VS_2, VSe_2, NbS_2 and $NbSe_2$ sheets),[9–11] MXenes (Ti_2C, V_2C, Cr_2C, Nb_2C, Zr_2C, Hf_2C and Ta_2C sheets),[12,13] organo-metal porous materials (Co-PP, Cr-PP, Cu-PP, Fe-PP, Mn-PP, Ni-PP and Zn-PP sheets),[14,15] metal-halides[16] and metal-oxides,[17,18] have been reported theoretically and experimentally. Among these, all IVA, IIIA, VA, IIIA–VA, IVA–VIA groups and most transition metal dichalcogenides in their pristine forms are nonmagnetic, thus hindering their applications in spin-based devices. Great efforts have been made in order to explore the application of 2D structures in this field.[19–27] For example, creating carbon vacancies in graphene,[19] doping metallic or nonmetallic atoms in graphene,[20,21] silicone,[22] germanene[22] and phosphorene,[23] and using strain in defect-interacted MoS_2 sheet,[25] have been confirmed as effective methods to generate spin. Particularly, FM, the important property for the application of 2D materials in spintronic devices, was predicted in half-brominated silicone[26] and half-fluorinated BN and ZnO sheets.[27] Nevertheless, experimental realisation of promising spin with the methods mentioned above still is difficult because precise modulations of vacancy, doping, strain and surface-functionalization on 2D structures is still challenging. Recently, there has been an increasing interest for exploring 2D structures with intrinsic magnetism.[28–31] Some MXenes,[28] organo-metallic porous sheets,[29] metal-halide sheets[30] and metal-oxide sheets[31] have been identified as excellent spin materials. In particular, robust FM was reported in pristine Ti_2C,[32] Ti_2N,[32] Cr_2C,[33] FeC_2,[34] VCl_3,[35] VI_3 (ref. 35) and $NiCl_3$ (ref. 36) sheets. While great efforts have been made in previous studies, researching new promising 2D spin structures is still important for further development of paper-like spin devices.

School of Physical Electronics, University of Electronic Science and Technology of China, Chengdu, 610054, P. R. China. E-mail: zhouyungang1@126.com; xiaxiang@uestc.edu.cn

† Electronic supplementary information (ESI) available. See DOI: 10.1039/c7ra02218b

$NiCl_2$ and $NiBr_2$ crystals have been prepared for several years with methods such as vapor phase dynamical transport method,[37] laser beam[38,39] and thermal evaporation.[40] It should be noted that $NiCl_2$ and $NiBr_2$ crystals are formed by the stacking of layers with the interlayer separations of 3.08 and 3.24 Å, respectively. The existence of large interlayer separation in such two materials provides a possibility of their exfoliations into single-layer sheets, as reported in graphene[1] and MoS_2.[9] Thus, in this study, we focused on the study of stability, geometrical structure, electronic and magnetic properties of $NiCl_2$ and $NiBr_2$ sheets. As mentioned above, $NiCl_2$ and $NiBr_2$ sheets can be viewed as 2D counterparts of $NiCl_2$ and $NiBr_2$ crystals, respectively.[41] Our paper is organized as follows: (1) we first discuss the geometric structures of $NiCl_2$ and $NiBr_2$ sheets; (2) the stabilities of $NiCl_2$ and $NiBr_2$ sheets are then examined by performing phonon dispersion curve calculations; (3) next, magnetic properties of $NiCl_2$ and $NiBr_2$ sheets, including magnetic moment, magnetic coupling, exchange parameter and Curie temperature, are studied in detail; (4) finally, based on the calculations of DOS and band structures, we analyze the electronic properties of $NiCl_2$ and $NiBr_2$ sheets; (5) in addition, we also explore the effect of strain on the magnetic properties of $NiCl_2$ and $NiBr_2$ sheets. Our aim in so doing is to assess the suitability of $NiCl_2$ and $NiBr_2$ sheets as excellent spin materials.

Theory and methods

First principles calculations were performed using projector augmented wave (PAW) type potentials[42] executed in the Vienna *ab initio* Simulation Package (VASP).[43,44] The Perdew–Burke–Ernzerhof (PBE)[45] pseudo potential inside the general gradient approximation (GGA) was chosen for the exchange correlation. The $3s^2 3p^5$, $4s^2 4p^5$ and $3d^8 4s^2$ atomic orbitals are treated as valence states for Cl, Br and Ni atoms, respectively. A plane wave basis set with threshold value of 600 eV was used. In order to avoid the interactions between neighboring sheets, we set a vacuum space of about 17 Å for $NiCl_2$ and $NiBr_2$ sheets. The *k*-point sampling in reciprocal space was represented with $10 \times 10 \times 1$ grid meshes. The convergence criterion for the atomic position and lattice vector optimizations was set as 1×10^{-4} eV in energy. To account for strong correlation of the unfilled d orbitals of the Ni atom, the *U* scheme was used to respect on-site electron correlation. Herein, the effective Coulomb exchange interaction, $U_{eff} = U - J$, where *U* and *J* are on-site Coulomb energy and exchange energy parameters, respectively, was set as 3 eV. The veracity of $U_{eff} = 3$ eV for 3d transition metal compounds has been confirmed in previous studies.[46,47] Moreover, in this study, the spin-resolved total DOS, atom projected density of states (PDOS) and band structure calculations were performed with a more accurate and reliable Heyd–Scouseria–Ernzerhof (HSE06) scheme.[48,49]

Results and discussions

We first performed the structural relaxations, including volume and atom position, for NiX_2 (X = Cl, Br) sheets. A 2×2 supercell that contains four Ni atoms and eight X atoms was applied for NiX_2 sheets. The optimized atomic structures of NiX_2 sheets are shown in Fig. 1. NiX_2 sheets show a close resemblance in structure with 1T-MoS_2.[50] Calculated lattice constants are about 3.50 and 3.70 Å for $NiCl_2$ and $NiBr_2$ sheets, respectively, which are comparable to the values of 3.48 and 3.72 Å for $NiCl_2$ and $NiBr_2$ in their bulk structures.[51,52] The "thickness" of $NiCl_2$ and $NiBr_2$ sheets are found to be about 2.69 and 2.85 Å, respectively, which also are comparable to the values of 2.72 and 2.87 Å for $NiCl_2$ and $NiBr_2$ in their bulk structures.[51,52] In addition, we found that the Cl–Ni–Cl bond angle in $NiCl_2$ sheet is about 92.80°, which is only 1.18° larger than the value of 91.62° found in its bulk structure; the calculated Br–Ni–Br bond angle in $NiBr_2$ sheet is about 92.17°, which is only 0.07° larger than the value of 92.10° found in its bulk structure.[51,52] Thus, the difference of structural parameters between 2D and their 3D

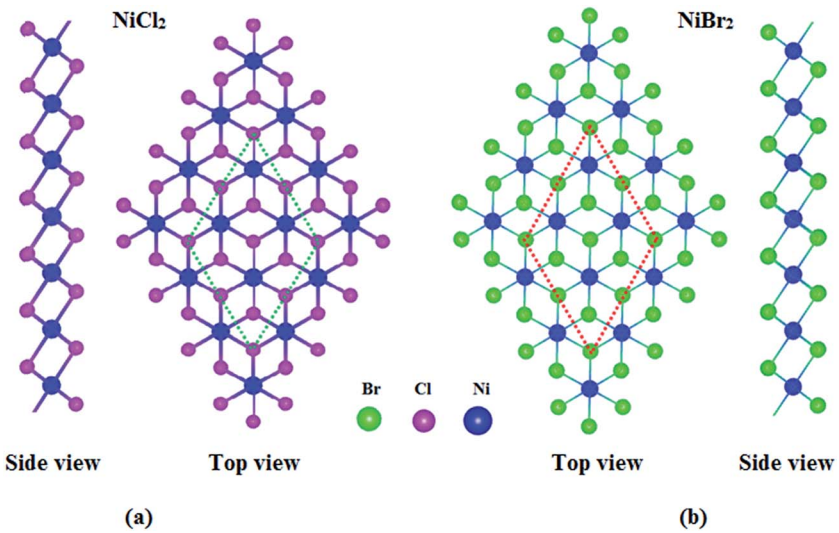

Fig. 1 Optimized geometric structures of (a) $NiCl_2$ and (b) $NiBr_2$ sheets. The selected 2×2 supercell is marked by the dotted lines.

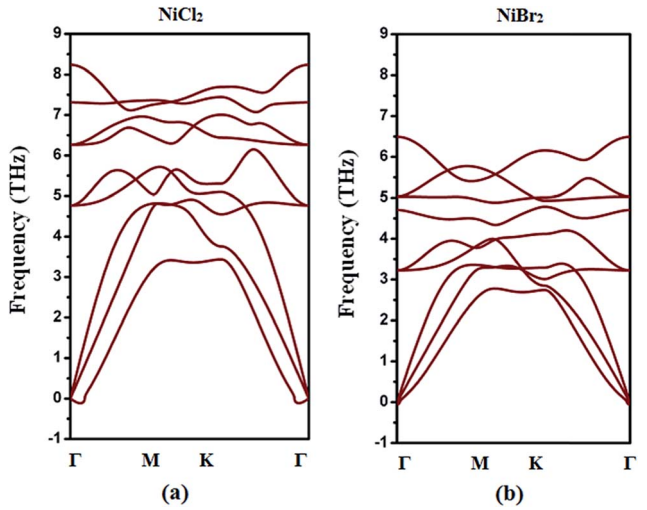

Fig. 2 The phonon dispersion curves of (a) $NiCl_2$ and (b) $NiBr_2$ sheets.

structures is very small, indicating that geometries of $NiCl_2$ and $NiBr_2$ sheets obtained from their bulk counterparts are well kept.

The stabilities of the structures are important for their practical applications. To check whether $NiCl_2$ and $NiBr_2$ sheets are stable enough, we performed phonon dispersion curve calculations. During the calculations a 1×1 unit cell was used for both cases. Since per unit cell contains three atoms (1Ni atom and 2X atoms), 9 phonon branches (3 acoustic branches and 6 optical branches) were observed in Fig. 2. Clearly, for $NiBr_2$ sheet, we found that there are no imaginary bands. Thus, $NiBr_2$ sheet is dynamically stable. As for $NiCl_2$ sheet, the lowest transverse branch has quite few imaginary frequencies as $\Gamma \rightarrow 0$. Nevertheless, we also conclude that $NiCl_2$ sheet is dynamically stable for two reasons: (1) the obtained imaginary frequencies might arise from the numerical artifacts because phonon dispersion calculations are highly sensitive to the choices of parameter and supercell and[36,53] (2) the obtained imaginary frequencies might be of acoustic nature because they are derived from a collective vibration mode with a long wavelength.[36,54]

Next, we carried out spin-polarized calculations to study the magnetic properties of NiX_2 sheets. In order to decide the most favorable state, a 2×2 supercell consisting of four Ni and eight X atoms was used. Three different coupling structures, including FM, AFM and nonmagnetic (NM) structures, were considered as shown in Fig. 3(a). Our calculations showed that for both structures, NM coupling is the least stable coupling, and FM coupling is somewhat more stable than AFM coupling. Calculated energy differences between AFM and FM couplings, $\Delta E = E_{AFM} - E_{FM}$, are about 63 and 71 meV for $NiCl_2$ and $NiBr_2$ sheets, respectively. Calculated net magnetic moment for $NiCl_2$ unit cell is about 1.91 μ_B, in which each Ni atom contributes 1.57 μ_B and each Cl atom contributes 0.16 μ_B; calculated net magnetic moment for $NiBr_2$ unit cell is about 1.88 μ_B, in which each Ni atom contributes 1.50 μ_B and each Br atom contributes 0.18 μ_B. Corresponding spin charge distributions for $NiCl_2$ and $NiBr_2$ sheets with FM coupling are shown in Fig. 3(b). Long-range magnetic ordering observed here makes $NiCl_2$ and $NiBr_2$ sheets promising candidates for spin applications. In order to estimate the robustness of FM coupling, we calculated the values of the exchange parameter J and Curie temperature

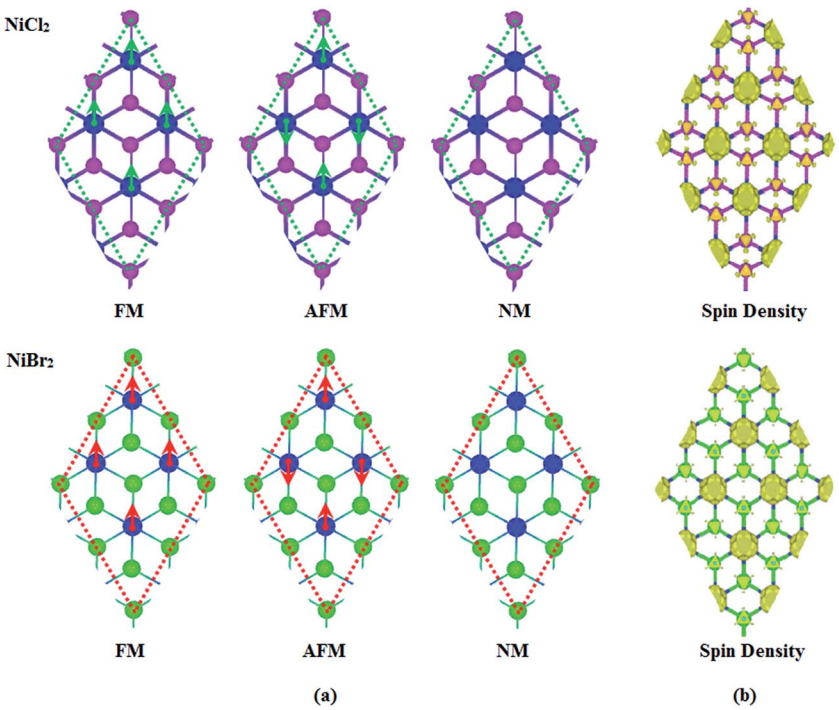

Fig. 3 (a) Ferromagnetic, antiferromagnetic, nonmagnetic configurations for $NiCl_2$ and $NiBr_2$ sheets. (b) The spin density distributions for ferromagnetic $NiCl_2$ and $NiBr_2$ sheets.

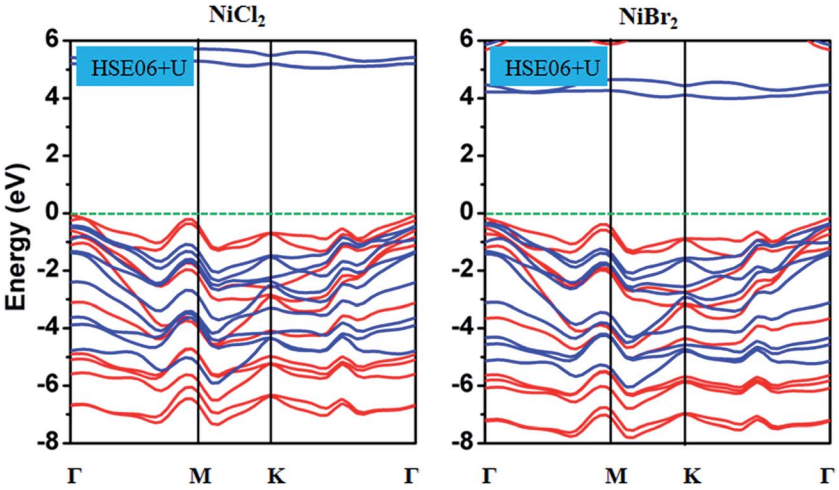

Fig. 4 Spin-polarized HSE06 + U band structures of $NiCl_2$ and $NiBr_2$ sheets. The red and blue solid lines correspond to the spin-up and spin-down states.

T_c. The value of J was obtained from the Ising model with the expression $H = -J\sum m_i m_j$, where H is the Hamiltonian in the absence of external magnetic field, J is the exchange parameter for two nearest neighbor Ni atoms located at sites i and j, and m_i and m_j are the magnetic moments of Ni atoms at sites i and j, respectively.[14] For $NiCl_2$ and $NiBr_2$ sheets, J can be represented as $J = \Delta E/16m^2$.[14,55] Calculated values of J are about 1.59 and 1.94 meV for $NiCl_2$ and $NiBr_2$ sheets, respectively. The positive sign of the constants confirm that Ni atoms in both cases prefer to be formed as FM coupling instead of AFM coupling. Furthermore, comparing with the values of other dihalides, such as 0.63 meV in $CrCl_3$ sheet and 0.81 meV in $CrBr_3$ sheet,[30] we believe the J values obtained here are large enough. The value of T_c was further evaluated based on a classical Heisenberg model with

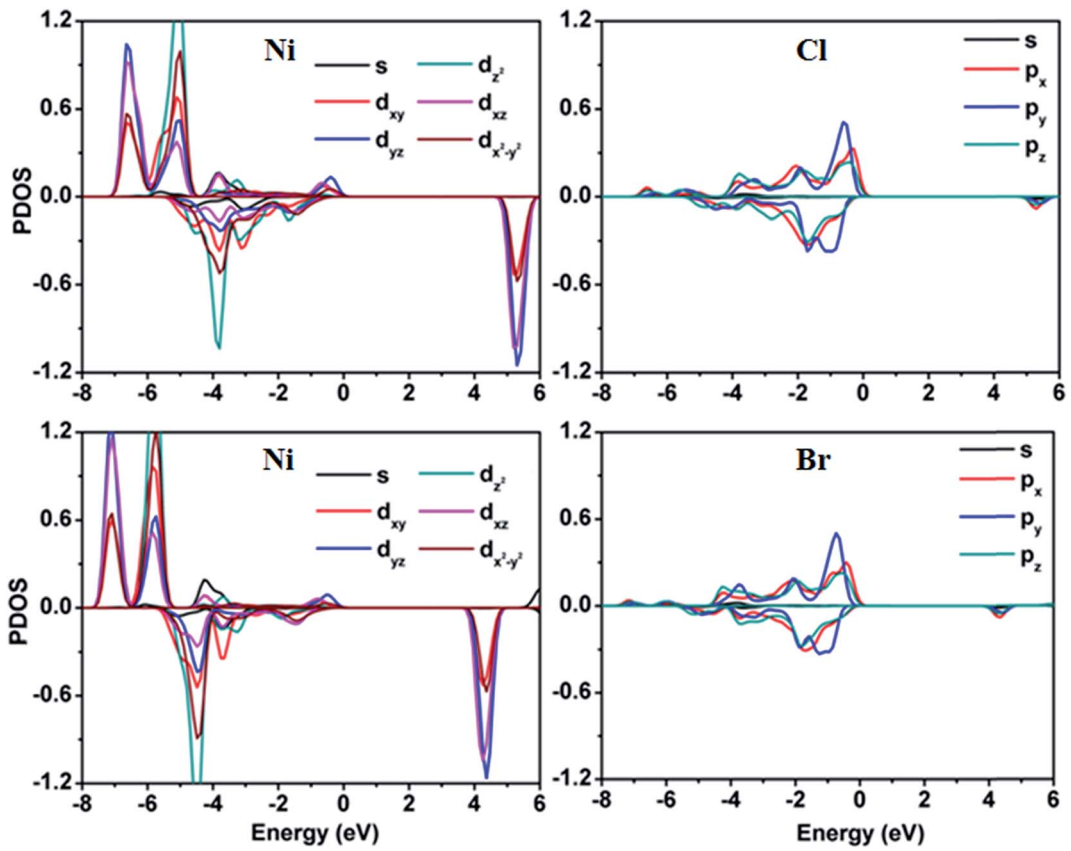

Fig. 5 Spin-polarized partial density of states of Ni and Cl atoms in $NiCl_2$ sheet and Ni and Br atoms in $NiBr_2$ sheet.

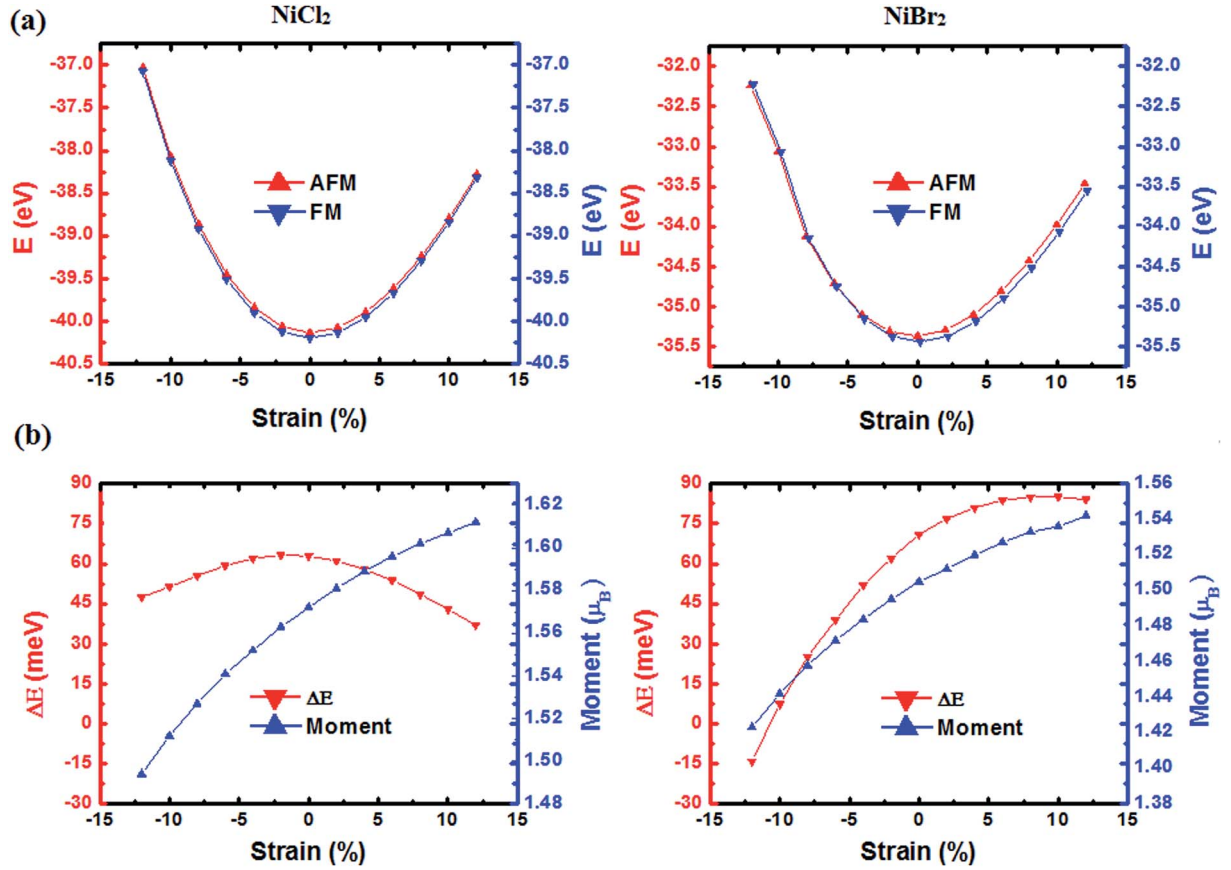

Fig. 6 (a) Change of total energies of ferromagnetic and antiferromagnetic $NiCl_2$ and $NiBr_2$ sheets with strain. (b) The changes of energy difference between AFM and FM couplings and magnetic moment of Ni atom with strain for $NiCl_2$ and $NiBr_2$ sheets.

the formula $T_c = 2/3(\Delta E/k_\beta)$,[56] where k_β is the Boltzmann constant. Calculated values of T_c are about 121 and 136 K for $NiCl_2$ and $NiBr_2$ sheets, respectively. Comparing with the values of 66 K reported in $CrCl_3$ sheet and 86 K reported in $CrBr_3$ sheet,[30] the obtained values of T_c here are also somewhat higher.

Finally, we explored the electronic properties of $NiCl_2$ and $NiBr_2$ sheets. Spin-polarized band structures based on HSE06 functional are shown in Fig. 4. Two important features were observed for $NiCl_2$ and $NiBr_2$ sheets. First, both sheets present a semiconducting property. Calculated band gaps are about 5.0 and 4.0 eV for $NiCl_2$ and $NiBr_2$ sheets, respectively. For both structures, the valence band maximum (VBM) and conduction band minimum (CBM) are contributed by spin-up and spin-down channels, respectively. In order to understand the origin of VBM and CBM, PDOS of Ni and Cl atoms in $NiCl_2$ sheet and Ni and Br atoms in $NiBr_2$ sheet were calculated, as shown in Fig. 5. It can be seen that for $NiCl_2$ sheet, the VBM mainly comes from the Cl atom and the CBM mainly comes from the Ni atom, and for $NiBr_2$ sheet, VBM mainly comes from the Br atom and the CBM mainly comes from the Ni atom. Further studies showed that VBM and CBM in $NiCl_2$ sheet are caused by the Cl-3p and Ni-3d orbitals, respectively, and VBM and CBM in $NiBr_2$ sheet are caused by the Br-4p and Ni-3d orbitals, respectively. In addition, we also calculated the band structures of $NiCl_2$ and $NiBr_2$ sheets with different U_{eff}, shown in Fig. 1S in the ESI.† Clearly, the change of band structure for both structures is very small with the increase of U_{eff}, indicating that the semiconducting property with large band gap found in $NiCl_2$ and $NiBr_2$ sheets is rather strong. Second, as shown in Fig. 4, a distinct asymmetry between the spin-up and spin-down channels was observed for $NiCl_2$ and $NiBr_2$ sheets. The asymmetry of spin channels mainly comes from the bands located at the energy region from −8.0 to 0 eV for both sheets. As shown in Fig. 5, we found that Ni atoms have a dominant contribution in the introduction of asymmetry of spin channels, and the contributions of Cl/Br atoms are small. Thus, for both sheets, the moment was caused mainly by Ni atoms, in accord with the moment calculations mentioned above. Further examination reveals that all d orbitals including d_{xy}, d_{yz}, d_{z^2}, d_{xz} and $d_{x^2-y^2}$ orbitals contribute to the magnetism for both sheets. As a result, the solid semiconductor and remarkable magnetism show great potential for the application of $NiCl_2$ and $NiBr_2$ sheets in the spin field.

It has been proven that the magnetic property of materials can be tuned by strain.[57] Thus, we also investigated the strain effect on the magnetic properties of $NiCl_2$ and $NiBr_2$ sheets by varying the biaxial strain from −12–12%. As shown in Fig. 6(a), total energies of $NiCl_2$ and $NiBr_2$ sheets increase continuously with the increase of tensile strain or compression strain, indicating that fracture

process will not happen when $NiCl_2$ and $NiBr_2$ sheets are deformed. Variations of the spin moment and the energy difference between AFM and FM states, ΔE, as a function of strain are shown in Fig. 6(b). One can see that the responses of ΔE against the strain for $NiCl_2$ and $NiBr_2$ sheets are somewhat different. For $NiCl_2$ sheet, the ΔE first increases and then decreases with the increase of strain, and for $NiBr_2$ sheet, the ΔE presents a tendency towards monotonic increase. Nevertheless, except for 12% compression strain applied in $NiBr_2$ sheet, ΔE is always positive for both cases, indicating that FM coupling is more stable than AFM coupling for different deformed structures. Moreover, for both cases, the moment increases almost linearly as we increase the strain. For $NiCl_2$ sheet, the moment increases from 1.49 to 1.61 μ_B when the strain increased from −12–12%, and, for $NiBr_2$ sheet, the moment increases from 1.42 to 1.54 μ_B when the strain increased from −12–12%. In addition, we also calculated their band structures with different strains, as shown in Fig. 2S in the ESI.† The change of band structure is very small with the increase of strain for both structures. Tunable magnetism and stable FM coupling and the semiconducting property indicate great potential applications of $NiCl_2$ and $NiBr_2$ in flexible spin nanoelectronics.

Conclusions

In conclusion, using DFT, we constructed NiX_2 (X = Cl, Br) sheets and studied their geometrical structures, stabilities, electronic and magnetic properties. Both sheets show a tri-layered structure in which the central layer is formed by Ni atoms and the top and bottom layers are formed by X atoms. The phonon dispersion calculations show that ultrathin NiX_2 structures are dynamically stable. Spin polarized calculations revealed that FM coupling is the ground state for NiX_2 sheets. Calculated energy differences between AFM and FM couplings are about 63 and 71 meV for $NiCl_2$ and $NiBr_2$ sheets, respectively. The spin-polarized DOS and band structure calculations based on HSE06 functional revealed that both sheets are solid semiconductors with remarkable magnetisms. In addition, strain effect calculations show that FM coupling is always more stable than AFM coupling for $NiCl_2$ and $NiBr_2$ sheets, and the moments of $NiCl_2$ and $NiBr_2$ sheets can be effectively tuned by applying biaxial strain. These results open the possibility for two new promising 2D structures in the application of spin devices.

Acknowledgements

This project was supported by the National Natural Science Foundation of China (No. 11504044), the Fundamental Research Funds for the Central Universities (No. ZYGX2015-KYQD012) and the New Academic Researcher Award (No. Y03111023901014002).

References

1 K. S. Novoselov, A. K. Geim, S. V. Morozov, D. Jiang, Y. Zhang, S. V. Dubonos, I. V. Grigorieva and A. A. Firsov, *Science*, 2004, **306**, 666–669.
2 H. Şahin, S. Cahangirov, M. Topsakal, E. Bekaroglu, E. Akturk, R. T. Senger and S. Ciraci, *Phys. Rev. B: Condens. Matter Mater. Phys.*, 2009, **80**, 155453.
3 H. Tang and S. Ismail-Beigi, *Phys. Rev. B: Condens. Matter Mater. Phys.*, 2010, **82**, 115412.
4 H. Liu, A. T. Neal, Z. Zhu, Z. Luo, X. Xu, D. Tománek and P. D. Ye, *ACS Nano*, 2014, **8**, 4033–4041.
5 S. Zhang, Z. Yan, Y. Li, Z. Chen and H. Zeng, *Angew. Chem., Int. Ed.*, 2015, **54**, 3112–3115.
6 C. Jin, F. Lin, K. Suenaga and S. Iijima, *Phys. Rev. Lett.*, 2009, **102**, 195505.
7 R. Ponce-Perez, G. H. Cocoletzi and N. Takeuchi, *J. Mol. Model.*, 2016, **22**, 226.
8 L. C. Gomes, A. Carvalho and A. H. Castro Neto, *Phys. Rev. B: Condens. Matter Mater. Phys.*, 2015, **92**, 214103.
9 K. S. Novoselov, D. Jiang, F. Schedin, T. J. Booth, V. V. Khotkevich, S. V. Morozov and A. K. Geim, *Proc. Natl. Acad. Sci. U. S. A.*, 2005, **102**, 10451–10453.
10 M. Chhowalla, H. S. Shin, G. Eda, L.-J. Li, K. P. Loh and H. Zhang, *Nat. Chem.*, 2013, **5**, 263–275.
11 J. N. Coleman, M. Lotya, A. O'Neill, S. D. Bergin, P. J. King, U. Khan, K. Young, A. Gaucher, S. De, R. J. Smith, I. V. Shvets, S. K. Arora, G. Stanton, H.-Y. Kim, K. Lee, G. T. Kim, G. S. Duesberg, T. Hallam, J. J. Boland, J. J. Wang, J. F. Donegan, J. C. Grunlan, G. Moriarty, A. Shmeliov, R. J. Nicholls, J. M. Perkins, E. M. Grieveson, K. Theuwissen, D. W. McComb, P. D. Nellist and V. Nicolosi, *Science*, 2011, **331**, 568–571.
12 M. Khazaei, M. Arai, T. Sasaki, C. Y. Chung, N. S. Venkataramanan, M. Estili, Y. Sakka and Y. Kawazoe, *Adv. Funct. Mater.*, 2013, **23**, 2185–2192.
13 G. Gao, G. Ding, J. Li, K. Yao, M. Wu and M. Qian, *Nanoscale*, 2016, **8**, 8986–8994.
14 J. Tan, W. Li, X. He and M. Zhao, *RSC Adv.*, 2013, **3**, 7016.
15 M. Abel, S. Clair, O. Ourdjini, M. Mossoyan and L. Porte, *J. Am. Chem. Soc.*, 2011, **133**, 1203–1205.
16 J. He, S. Ma, P. Lyu and P. Nachtigall, *J. Mater. Chem. C*, 2016, **4**, 2518–2526.
17 M. Topsakal, S. Cahangirov, E. Bekaroglu and S. Ciraci, *Phys. Rev. B: Condens. Matter Mater. Phys.*, 2009, **80**, 235119.
18 M. Kan, J. Zhou, Q. Sun, Y. Kawazoe and P. Jena, *J. Phys. Chem. Lett.*, 2013, **4**, 3382–3386.
19 M. M. Ugeda, I. Brihuega, F. Guinea and J. M. Gomez-Rodriguez, *Phys. Rev. Lett.*, 2010, **104**, 096804.
20 E. J. G. Santos, A. Ayuela and D. Sánchez-Portal, *New J. Phys.*, 2010, **12**, 053012.
21 L. Xie, X. Wang, J. Lu, Z. Ni, Z. Luo, H. Mao, R. Wang, Y. Wang, H. Huang, D. Qi, R. Liu, T. Yu, Z. Shen, T. Wu, H. Peng, B. Ozyilmaz, K. Loh, A. T. S. Wee, Ariando and W. Chen, *Appl. Phys. Lett.*, 2011, **98**, 193113.
22 X. Q. Wang, H. D. Li and J. T. Wang, *Phys. Chem. Chem. Phys.*, 2012, **14**, 3031–3036.
23 H. Zheng, J. Zhang, B. Yang, X. Du and Y. Yan, *Phys. Chem. Chem. Phys.*, 2015, **17**, 16341–16350.
24 A. Ramasubramaniam and D. Naveh, *Phys. Rev. B: Condens. Matter Mater. Phys.*, 2013, **87**, 195201–195207.

25 P. Tao, H. Guo, T. Yang and Z. Zhang, *J. Appl. Phys.*, 2014, **115**, 054305.
26 F.-B. Zheng and C.-W. Zhang, *Nanoscale Res. Lett.*, 2012, **7**, 422.
27 E. J. Kan, H. J. Xiang, F. Wu, C. Tian, C. Lee, J. L. Yang and M. H. Whangbo, *Appl. Phys. Lett.*, 2010, **97**, 122503.
28 S. Zhao, W. Kang and J. Xue, *Appl. Phys. Lett.*, 2014, **104**, 133106.
29 E. Kan, X. Wu, C. Lee, J. H. Shim, R. Lu, C. Xiao and K. Deng, *Nanoscale*, 2012, **4**, 5304–5307.
30 J. Liu, Q. Sun, Y. Kawazoe and P. Jena, *Phys. Chem. Chem. Phys.*, 2016, **18**, 8777–8784.
31 W. Cheng, J. He, T. Yao, Z. Sun, Y. Jiang, Q. Liu, S. Jiang, F. Hu, Z. Xie, B. He, W. Yan and S. Wei, *J. Am. Chem. Soc.*, 2014, **136**, 10393–10398.
32 G. Gao, G. Ding, J. Li, K. Yao, M. Wu and M. Qian, *Nanoscale*, 2016, **8**, 8986–8994.
33 C. Si, J. Zhou and Z. Sun, *ACS Appl. Mater. Interfaces*, 2015, **7**, 17510–17515.
34 T. Zhao, J. Zhou, Q. Wang, Y. Kawazoe and P. Jena, *ACS Appl. Mater. Interfaces*, 2016, **8**, 26207–26212.
35 J. He, S. Ma, P. Lyua and P. Nachtigall, *J. Mater. Chem. C*, 2016, **4**, 2518–2526.
36 J. He, X. Li, P. Lyu and P. Nachtigall, *Nanoscale*, 2017, **9**, 2246–2252.
37 M. Kozielski, I. Pollini and G. Spinolo, *J. Phys. C: Solid State Phys.*, 1972, **5**, 1253.
38 H. Y. Rosenfeld, R. Popovitz-Biro, Y. Prior, S. Gemming, G. Seifert and R. Tenne, *Phys. Chem. Chem. Phys.*, 2003, **5**, 1644–1651.
39 H. Y. Rosenfeld, R. Popovitz-Brio, E. Grunbaum, Y. Prior and R. Tenne, *Adv. Mater.*, 2002, **14**, 1075–1078.
40 M. Bar-Sadan, R. Popovitz-Biro, Y. Prior and R. Tenne, *Mater. Res. Bull.*, 2006, **41**, 2137–2146.
41 M. R. Tubbs, *Phys. Status Solidi B*, 1972, **49**, 11–50.
42 P. E. Blöchl, *Phys. Rev. B: Condens. Matter Mater. Phys.*, 1994, **50**, 17953–17979.
43 G. Kresse and J. Hafner, *Phys. Rev. B: Condens. Matter Mater. Phys.*, 1993, **47**, 558–561.
44 G. Kresse and F. Jürgen, *Phys. Rev. B: Condens. Matter Mater. Phys.*, 1996, **54**, 11169.
45 J. P. Perdew, K. Burke and M. Ernzerhof, *Phys. Rev. Lett.*, 1996, **77**, 3865–3868.
46 H. S. Kim and H. Y. Kee, *Phys. Rev. B: Condens. Matter Mater. Phys.*, 2015, **92**, 235121.
47 M. Arita, K. Shimada, Y. Utsumi, O. Morimoto, H. Sato, H. Namatame, M. Taniguchi, Y. Hadano and T. Takabatake, *Phys. Rev. B: Condens. Matter Mater. Phys.*, 2011, **83**, 246116.
48 J. Heyd, G. E. Scuseria and M. Ernzerhof, *J. Chem. Phys.*, 2003, **118**, 8207–8215.
49 F. Fuchs, J. Furthmüller, F. Bechstedt, M. Shishkin and G. Kresse, *Phys. Rev. B: Condens. Matter Mater. Phys.*, 2007, **76**, 115109.
50 G. Eda, T. Fujita, H. Yamaguchi, D. Voiry, M. Chen and M. Chhowalla, *ACS Nano*, 2012, **6**, 7311–7317.
51 J. A. A. Ketelaar, *Z. Kristallogr.*, 1934, **88**, 26–34.
52 A. Ferrari, A. Braibanti and G. Bigliardi, *Acta Crystallogr.*, 1963, **16**, 846–847.
53 S. H. Lin and J. L. Kuo, *Phys. Chem. Chem. Phys.*, 2014, **16**, 20763–20771.
54 X. Li, Y. Dai, M. Li, W. Wei and B. Huang, *J. Mater. Chem. A*, 2015, **3**, 24055–24063.
55 J. Zhou and Q. Sun, *J. Am. Chem. Soc.*, 2011, **133**, 15113–15119.
56 Y. W. Ma, Y. H. Lu, J. B. Yi, Y. P. Feng, T. S. Herng, X. Liu, D. Q. Gao, D. S. Xue, J. M. Xue, J. Y. Ouyang and J. Ding, *Nat. Commun.*, 2012, **3**, 727.
57 J. Zhou, Q. Wang, Q. Sun, Y. Kawazoe and P. Jena, *J. Phys. Chem. Lett.*, 2012, **3**, 3109–3114.